Audio Engineering Society

Conference Paper 7

Presented at the AES 5th International Conference on Automotive Audio
2024 June 26–28, Gothenburg, Sweden

This paper was peer-reviewed as a complete manuscript for presentation at this conference. This paper is available in the AES E-Library (http://www.aes.org/e-lib), all rights reserved. Reproduction of this paper, or any portion thereof, is not permitted without direct permission from the Journal of the Audio Engineering Society.

Perceived spatial extent of local active noise control for broadband disturbances

Felix Holzmüller[1] and Alois Sontacchi[1]

[1] *Institute of Electronic Music and Acoustics, University of Music and Performing Arts Graz*

Correspondence should be addressed to Felix Holzmüller (holzmueller@iem.at)

ABSTRACT

This paper investigates the perceived spatial extent of a local active noise control system for different types of disturbances. Several publications determined size and shape of the zone of quiet for various arrangements through analytical and numerical methods. However, these studies have often overlooked human perception, focusing solely on technical properties. Therefore, a listening experiment has been conducted to determine the perceived size of the zone of comfort in a scenario close to reality, using an active headrest setup. Several operational frequency limits for different types and directions of broadband disturbances are examined. Within this experiment, lateral transitions to the front and head rotations at the target position have been considered. Statistically consolidated subjective ratings exhibit limits of around 2 cm to 4 cm for lateral transitions, with an expected decrease towards higher frequencies. When comparing participants' answers to measurements, the majority of the median responses converge at a point with loudness reduction of 20 %. The rotational limits of 7 ° to 15 ° are not as dependent on frequency, but are confined by the distinct perception of the secondary sources as well.

1 Introduction

Active noise control (ANC) is a technique for the reduction of unwanted disturbances. Most ANC algorithms are based on the same fundamental principle: capturing signals closely related to the disturbances, manipulating them with a control filter, and playing the signals back via loudspeakers, also called secondary sources in the context of active control. The filters are designed beforehand or adapted during operation to ensure that at one or more points of cancellation the sound pressure generated by the secondary sources accurately resembles the disturbances, but with inverted phase. This results in a reduction of the disturbances through destructive interference.

In an automotive scenario, active control can be used to reduce engine and road noise [1]. Unlike traditional passive noise reduction techniques such as structural optimisations or the addition of absorptive materials, ANC systems are generally capable of controlling lower frequencies while being lightweight and potentially utilising already installed sensors and transducers. Global ANC aims to reduce sound pressure throughout the entire space, while local ANC is optimised to reduce disturbances at specific positions. The latter approach extends the controlled bandwidth while requiring fewer secondary sources [1]. Although active headrests containing secondary loudspeakers have already been part of early ANC systems [2], they have gained popularity especially in recent years [3, 4, 5]. Ad-

vantages of these systems compared to door-mounted loudspeakers are faster convergence time and increased stability when using adaptive filters due to a smaller plant delay [6]. Although arrangement and geometry of the headrest have influence on the noise reduction performance [3], the results of this study can be an indicator for many similar cases.

Local ANC has a limited spatial extent. Various analytical and numerical studies have determined the *zone of quiet* (ZoQ), which refers to the the area where 10 dB noise reduction is achieved around the point of cancellation, for different scenarios. In a pure-tone diffuse sound field, the ZoQ takes the shape of a sphere with a diameter of approximately 1/10-th of the wavelength when using a single secondary source in the acoustic far-field [7]. Subsequent studies have expanded upon this research to include multiple points of cancellation [8] and broadband disturbances with secondary sources in both the acoustic near- and far-field [9]. However, the majority of these studies focus solely on unweighted sound pressure levels as performance measure, neglecting the role of human perception. Thus, this study presents results of a listening experiment that has been conducted to determine the *perceived* size of the controlled area, referred to as *zone of comfort* (ZoC), for various scenarios in a noise control setting close to reality. The results of this study can serve as a reference for perceptually optimised ANC systems, for example regarding the accuracy of head-tracking based approaches [10]. After a brief derivation of an optimal control filter in section 2, the experiment setup is described in section 3 while the results are presented in section 4. These results are then contextualised and compared to measurements and psychoacoustic measures in section 5. Recordings of all stimuli at various positions as well as the results of the listening experiment are openly accessible [11].

2 Optimal control filter

Fig. 1 shows a block diagram of the feedforward ANC system used in the experiment. For best noise reduction performance at the point of cancellation, an optimal, static control filter is used. While a comprehensive derivation for this filter is given for example by Elliott and Cheer [12], only a simplified version in the z-domain is provided in this publication, where for example $\mathbf{D}_e(z)$ corresponds to the z-transform of a discrete-time signal $\mathbf{d}_e[n]$.

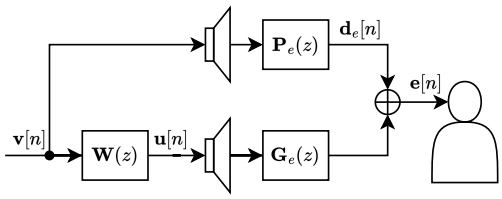

Fig. 1: Simplified block diagram of a feedforward ANC system with a static control filter.

Given the known transfer functions $\mathbf{P}_e(z)$ between the primary sources and the points of cancellation, the primary disturbances $\mathbf{D}_e(z)$ at the points of cancellation can be expressed as

$$\mathbf{D}_e(z) = \mathbf{P}_e(z)\mathbf{V}(z)\,, \tag{1}$$

where $\mathbf{V}(z)$ are the innovation signals driving the primary sources. For this experiment, the innovation signals are also used as the input of the control filter $\mathbf{W}(z)$ to avoid deteriorated performance due to low coherence between the primary disturbances and the control filter's input. The control signals $\mathbf{U}(z)$ driving the secondary sources are therefore defined as

$$\mathbf{U}(z) = \mathbf{W}(z)\mathbf{V}(z)\,. \tag{2}$$

The residual noise $\mathbf{E}(z)$ at the points of cancellation can now be found with

$$\mathbf{E}(z) = \mathbf{D}_e(z) + \mathbf{G}_e(z)\mathbf{U}(z) = \tag{3}$$

$$= \mathbf{P}_e(z)\mathbf{V}(z) + \mathbf{G}_e(z)\mathbf{W}(z)\mathbf{V}(z)\,, \tag{4}$$

where $\mathbf{G}_e(z)$ is a set of transfer functions between the secondary sources and the points of cancellation. With optimal noise control, the residual error $\mathbf{E}(z)$ should be equal to zero. Equation (4) can therefore be rewritten to

$$\mathbf{P}_e(z)\mathbf{V}(z) = -\mathbf{G}_e(z)\mathbf{W}_{\text{opt}}(z)\mathbf{V}(z)\,. \tag{5}$$

If $\mathbf{G}_e(z)$ is invertible, the optimal control filter can be calculated with

$$\mathbf{W}_{\text{opt}}(z) = -\mathbf{G}_e^{-1}(z)\mathbf{P}_e(z)\,. \tag{6}$$

3 Experiment setup

The listening experiment was conducted in an acoustically treated room with non-parallel walls and dimensions of approximately 5 m × 4 m × 3 m. The room has a reverberation time of less than 50 ms above 300 Hz

and less than 30 ms above 1 kHz. Within this space, eight Genelec 8020 B loudspeakers, arranged in a circular configuration with a radius of 1.5 m, serve as the primary sources of disturbances, as illustrated in Fig. 2. An active headrest prototype with two loudspeakers, placed approximately 20 cm apart and facing the listener's ears in resting position, is used as secondary source. The position of the participant is captured by a tracking system (OptiTrack Motive with 6 Flex3 cameras, mean error ≤ 0.4 mm) with an optical marker placed on the participant's head as shown in Fig. 3. To compensate for variations in marker placement, each participant has to find their reference position, the location with best noise attenuation, in a brief pre-trial.

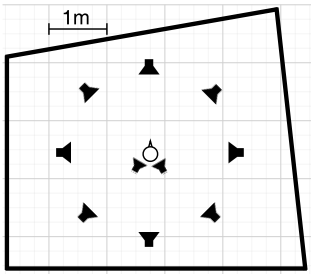

Fig. 2: Schematics of the room and loudspeaker arrangement.

In the listening experiment itself, participants are instructed to rotate (clockwise and counterclockwise) or move their head forward, starting at the reference position. When the perceived ZoC is left or the secondary sources are starting to cause additional disturbances, a button on a provided tablet PC should be pressed to capture the position. If this point cannot be found or is outside the range of motion, an "out of bounds" response can be given. In any case, playback of the primary disturbances and therefore also of the secondary signals is stopped after each response. The next trial starts immediately when the reference position is reached again with an accuracy of ± 1 cm and $\pm 3\,^{\circ}$. This procedure allows for identical starting conditions across trials. The tablet PC provides a user interface for instructions, visual feedback to find the reference position between trials faster, and a button to disable ANC temporarily as well. The display is mirrored to a second screen at eye level to keep the participant's head as straight as possible. Despite this measure, a noticeable change in pitch angle could be observed with some participants for lateral transition trials. Due to the fact that the optical marker for the tracking system is placed at the

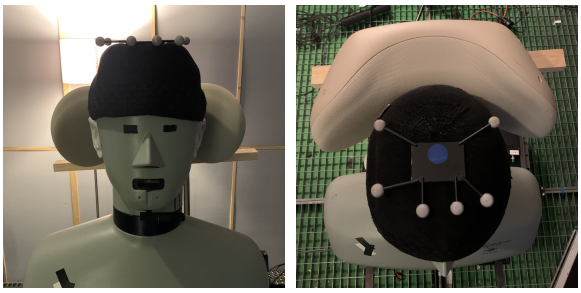

(a) Front view (b) Top view

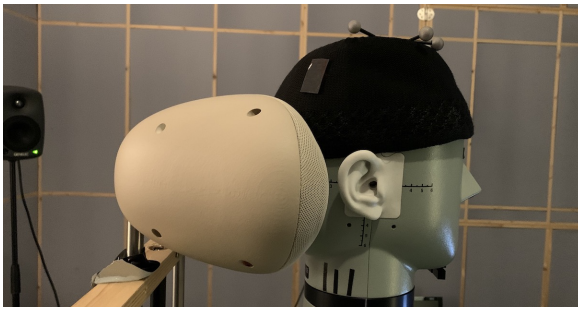

(c) Side view

Fig. 3: Positioning of the participant and tracking marker in front of an active headrest.

top of the participant's head and not at ear level (see Fig. 3), the recorded position has to be corrected to avoid exaggerated results. The corrected position in frontal direction is therefore

$$\widetilde{tr}_x = tr_x + os_z \cdot \sin(pitch), \tag{7}$$

where tr_x is the uncorrected position along the lateral plane and os_z the vertical offset between the tracking marker and the ear canal. A value of $os_z = 13$ cm is chosen, measured on a Brüel & Kjær 4128C head and torso simulator (HATS).

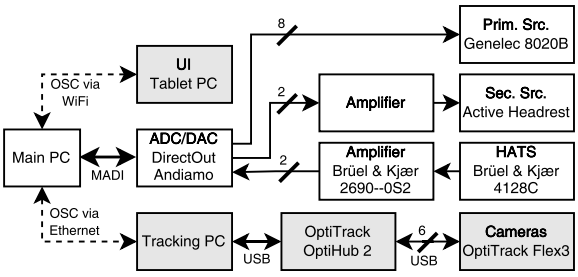

Fig. 4: Block diagram of the measurement setup.

Before calculating the control filter, all transfer paths between the primary and secondary loudspeakers and a HATS are measured using an exponential sweep method [13] at a sample rate of 44.1 kHz with the setup depicted in Fig. 4. To resemble a realistic scenario, the HATS is placed as close as possible to the active headrest without touching it to avoid mechanical coupling and structure-borne sound in measurements. With eight primary and two secondary sources, this results in a 2×8 matrix of primary paths $\mathbf{P}_e(z)$ and a 2×2 matrix of secondary paths $\mathbf{G}_e(z)$. The impulse responses are windowed to remove floor and wall reflections. For the experiment, the 2×8 static control filter $\mathbf{W}_{\text{opt}}(z)$ is calculated bin-wise in frequency domain [12] while ensuring a causally constrained filter design, following the formulation in eq. (6). The matrix $\mathbf{G}_e(z)$ was conditioned well enough to omit regularisation before inversion while still operating at the playback system's default sample rate of 44.1 kHz.

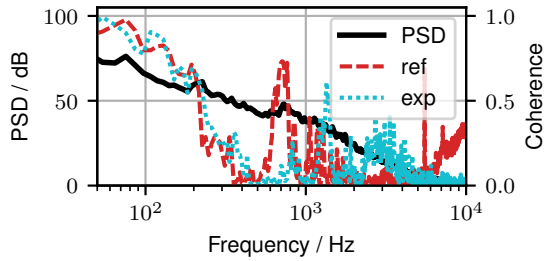

Fig. 5: Power spectral density (PSD) of the used in-car recording at 80 km/h, as well as the interaural coherence measured inside the vehicle (ref) and simulated in the experiment (exp).

Two different types of innovation signals are used in the experiment - uniform white noise, low-pass filtered with a 32nd Butterworth filter as done by Rafaely [9], and a recording of in-car noise (Audi A6 C6 Sedan, 3.0 TDI at 80 km/h speed) with the power spectral density shown in Fig. 5. The in-car noise is additionally tested for wide-sense stationarity [14]. Different upper operational frequency limits of the ANC algorithm are set to 500 Hz, 1 kHz, 2 kHz, and 10 kHz. To achieve this, the low-pass cut-off frequency of the white noise innovation signal is set to the corresponding value. For the in-car noise, the control filters themselves are post-processed with a 6th order Butterworth low-pass filter, using a zero-phase forward-backward approach [15] to preserve their phase response, while playing the unmodified primary disturbances in the experiment in all cases.

Primary disturbances are played either by a single loudspeaker in the front, in the rear or from all eight loudspeakers on the horizontal plane. To create a diffuse scenario for the latter, the mono innovation signals are processed with a granular synthesizer and encoded to the Ambisonic domain as proposed by Riedel et al. [16]. The signal is decoded to the loudspeakers using the AllRAD approach [17] with two zero-gain imaginary loudspeakers at $\pm 90\,^\circ$ elevation. The GranularEncoder and AllRADecoder of the IEM Plug-In Suite[1] are used for processing, all parameters deviating from their default values are listed in table 1. With this method, an interaural coherence comparable to reference recordings with a HATS in the vehicle is achieved below 500 Hz as shown in Fig. 5. All primary disturbances are levelled to approximately 58 dB(A) at the listening position, similar to the level in the car.

Parameter	Base value	Modulation
Grain length	0.841 s	31.5 %
Time between grains	0.001 s	
Buffer position	1.125 s	1.112 s
Max. spread	360 °	
Grain distribution	circular	

Table 1: Custom GranularEncoder settings.

Each combination of innovation signal, controlled frequency range and primary disturbance direction is presented once. One selected combination (white noise, low-pass cut-off frequency at 1 kHz, diffuse) is presented four times to assess reliability and consistency of the participants. This results in a total of 81 trials.

The white noise innovation signals and the control filters are calculated in advance in MATLAB. The central control of the experiment (stimulus selection, playback logic, export of results) is programmed in Pure Data[2]; MobMuPlat[3] [18] acts as user interface on the tablet PC. The audio signals are played back by the digital audio workstation REAPER, the control filter is applied with the mcfx VST2 plug-in[4]. All subsystems communicate via the Open Sound Control (OSC) protocol.

[1] https://plugins.iem.at/
[2] http://msp.ucsd.edu/software.html
[3] https://danieliglesia.com/mobmuplat/
[4] https://github.com/kronihias/mcfx

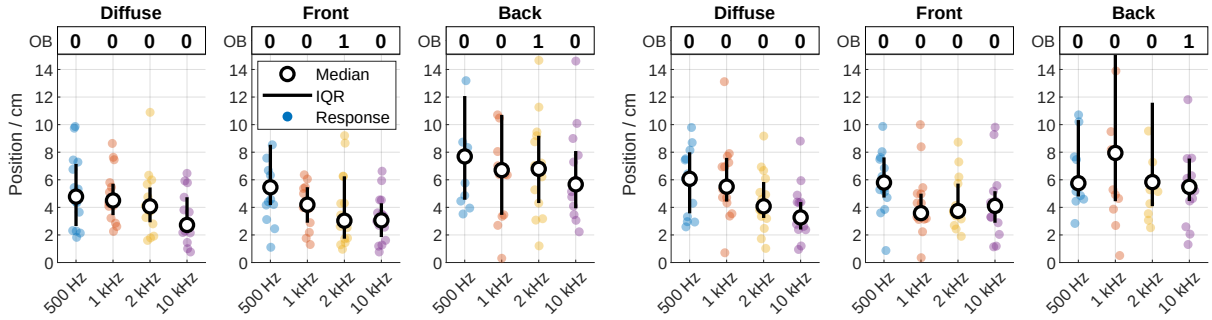

(a) White noise (b) In-car noise

Fig. 6: Median, range between first and third quartile (IQR), individual answers, and number of "out of bounds" (OB) for **transition** trials for different primary disturbance directions. The labels on the abscissa refer to the cut-off frequencies of the low-pass filter.

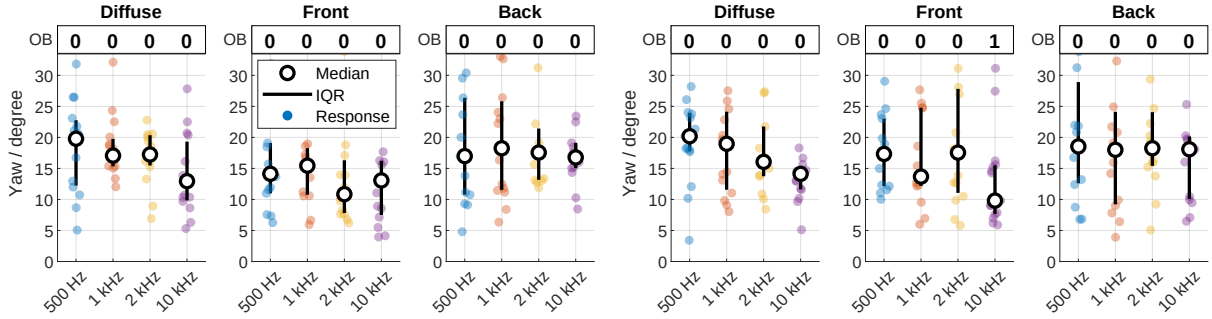

(a) White noise (b) In-car noise

Fig. 7: Median, range between first and third quartile (IQR), individual answers, and number of "out of bounds" (OB) for counterclockwise **rotation** trials for different primary disturbance directions. The labels on the abscissa refer to the cut-off frequencies of the low-pass filter.

4 Results

A total of 24 people between 21 and 60 years (29 years median) participated in the experiment, aiming to quantify perceived spatial limits of local ANC. 20 subjects have previously taken part in listening experiments, 22 have a self-reported background in acoustics and/or audio engineering. None reported any hearing impairment. Experiment durations ranging from 11 min to 64 min with a median of 21 min are recorded. Although with this number of participants differences between conditions are rarely statistically significant at $\alpha = 0.05$, certain trends can be identified based on median and quartile location.

A within-subject reliability index [19] is used to evaluate the consistency of responses. With the variance over the repeated trials σ^2_{rep} and the variance over all trials σ^2_{all}, it can be calculated as

$$r = 1 - \frac{\sigma^2_{\text{rep}}}{\sigma^2_{\text{all}}}. \tag{8}$$

Eight participants are excluded from further analysis based on a low reliability index of $r < 0.6$ and another person is excluded due to a strikingly high overall variance and multiple "out of bounds" answers in the repeated trials.

A Wilcoxon signed rank test [20] with Holm-Bonferroni correction [21] is performed to check for significant differences in responses for clockwise and counterclockwise rotation. With the exception of one condition (frontal in-car noise, cut-off frequency at

2 kHz), no significant differences are found at a significance level of $\alpha = 0.05$. However, for further analysis only counterclockwise rotation is considered, as this is the direction where the sound field has been recorded.

The results of the listening experiment are shown in Fig. 6 and 7. Similar tendencies and results can be observed for both low-pass filtered white noise and in-car noise. Especially in the transition trials, the perceived size of the ZoC decreases towards higher frequencies. This is not a surprise, as simulations by Rafaely [9] have shown that for diffuse band-pass filtered noise the ZoQ is similar to that of pure-tone disturbances at the mid-frequency of the noise bandwidth and shrinking towards higher frequencies. It is also evident, that the direction of the primary disturbances has influence on the size of the ZoC. While frontal and diffuse scenarios produce relatively similar results, larger ZoCs are seen for dorsal disturbances. This is in line with simulations by Elliott and Cheer [12], as the secondary sources are located behind the participant as well, resulting in a closer match of phase variation of primary and secondary sources in the examined direction. A higher interquartile range (IQR) for dorsal disturbances is also noticeable, which can be explained by a more gentle loudness increase compared to other directions (see Fig. 8 and section 5).

The first quartile acts as a general indicator for the size of the ZoC, defining an area that is valid for 75 % of participants. This threshold is easily identifiable in Fig. 6 and 7. For transition trials with frontal and diffuse disturbances, the ZoC has an extent of about 4 cm for lower cut-off frequencies with the aforementioned criterion, declining to about 2 cm towards higher frequencies. A plateau for the extent of the ZoC is reached at or slightly above 1 kHz cut-off frequency for frontal disturbances. Although the median of responses for dorsal disturbances declines towards higher frequencies, the first quartile remains relatively constant at 4 cm across all conditions.

The reduction of the median ZoC size towards higher cut-off frequencies can also be observed to a certain degree with diffuse and frontal disturbances during a rotational motion as shown in Fig. 7. However, for most dorsal and diffuse conditions, the lower quartile is located between 10 ° and 15 ° and relatively independent of controlled frequency. Frontal disturbances result in a slightly narrower ZoC ranging from 7 ° to 12 °.

5 Relation to perceived loudness

To understand why participants answered this way, primary and residual disturbances are evaluated further. The sound field with and without noise control is captured for every condition with a HATS at several lateral positions of $\{0, 3, 6, 9, 12, 15, 20, 25, 30\}$ cm and head rotations at the reference position of $\{0, 10, 20, 30, 40, 50\}^\circ$.

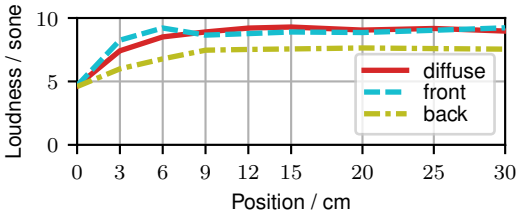

Fig. 8: Loudness of low-pass filtered white noise at 2 kHz cut-off frequency with ANC for several primary source directions during lateral transition.

Fig. 8 shows the binaural loudness according to Moore and Glasberg [22] for different primary disturbance directions with low-pass filtered white noise at 2 kHz cut-off frequency as example. In general, more increase in loudness near the reference position can be observed for frontal disturbances, whereas dorsal disturbances result in a slower increase and lower maximum loudness. The less steep loudness increase can account for the larger IQR of the responses for dorsal disturbances.

The noise reduction performance can provide an explanation to the general response behaviour of test subjects for transition trials. Fig. 9 shows the ratio between the loudness with and without ANC across all measured positions. Over all conditions, the first quartile of the responses is located on average at a noise reduction ratio of 0.82 with a standard deviation of 0.07, indicating a perceived loudness reduction by approximately 20 % caused by the ANC system. However, there are some outliers to this observation, such as for cut-off frequencies at 10 kHz in Fig. 9(a) and 9(e) or 500 Hz in Fig. 9(f). In these scenarios, notably less noise reduction is exhibited at the reference position, almost moving the noise reduction ratio parallelly throughout the examined range. For frontal disturbances in Fig. 9(c) and 9(d), the median response is notably higher at a noise reduction ratio of almost 1, indicating the same

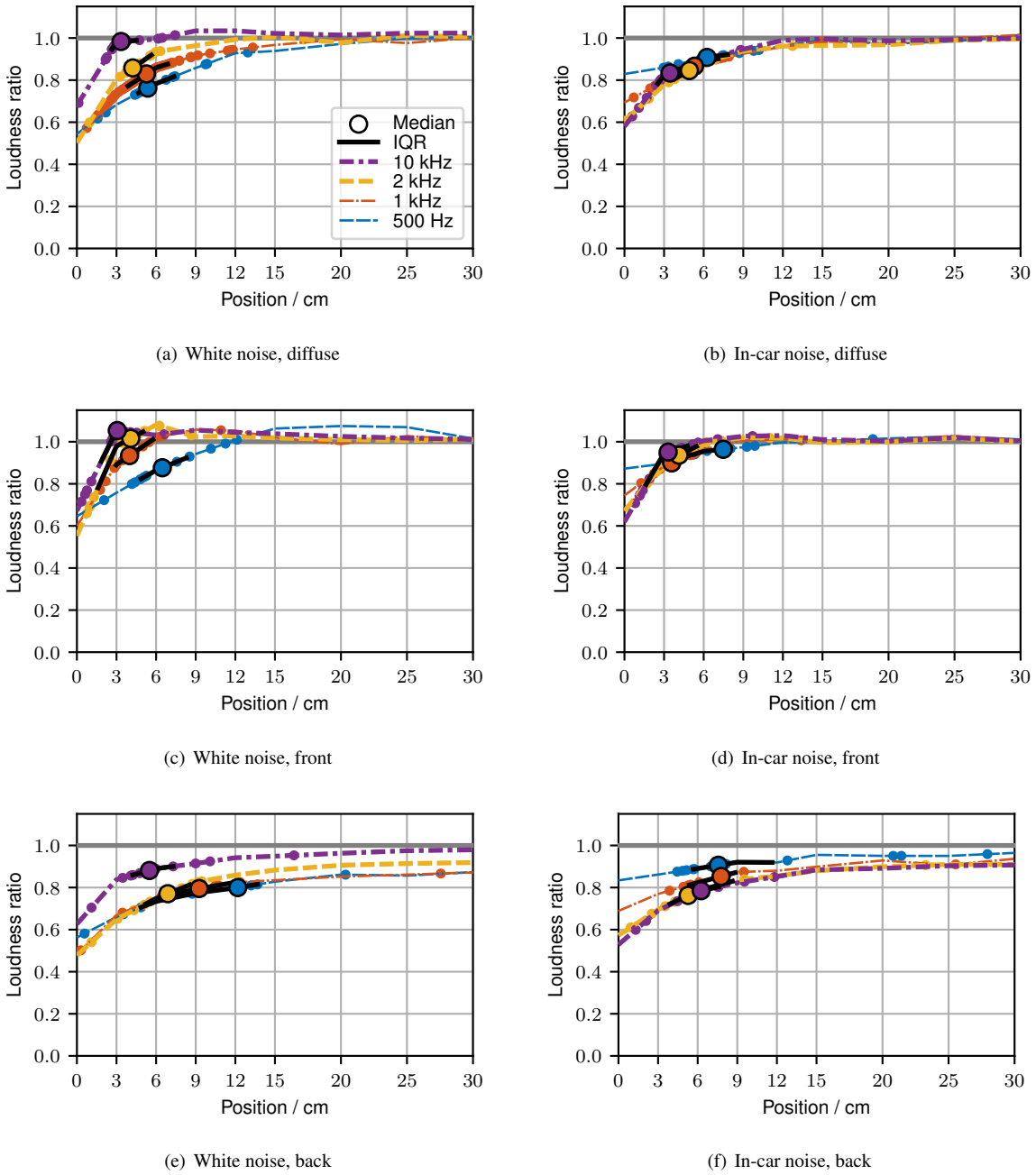

(a) White noise, diffuse

(b) In-car noise, diffuse

(c) White noise, front

(d) In-car noise, front

(e) White noise, back

(f) In-car noise, back

Fig. 9: Relative loudness reduction for different positions and cut-off frequencies. Median, range between first and third quartile (IQR), and individual responses are overlaid.

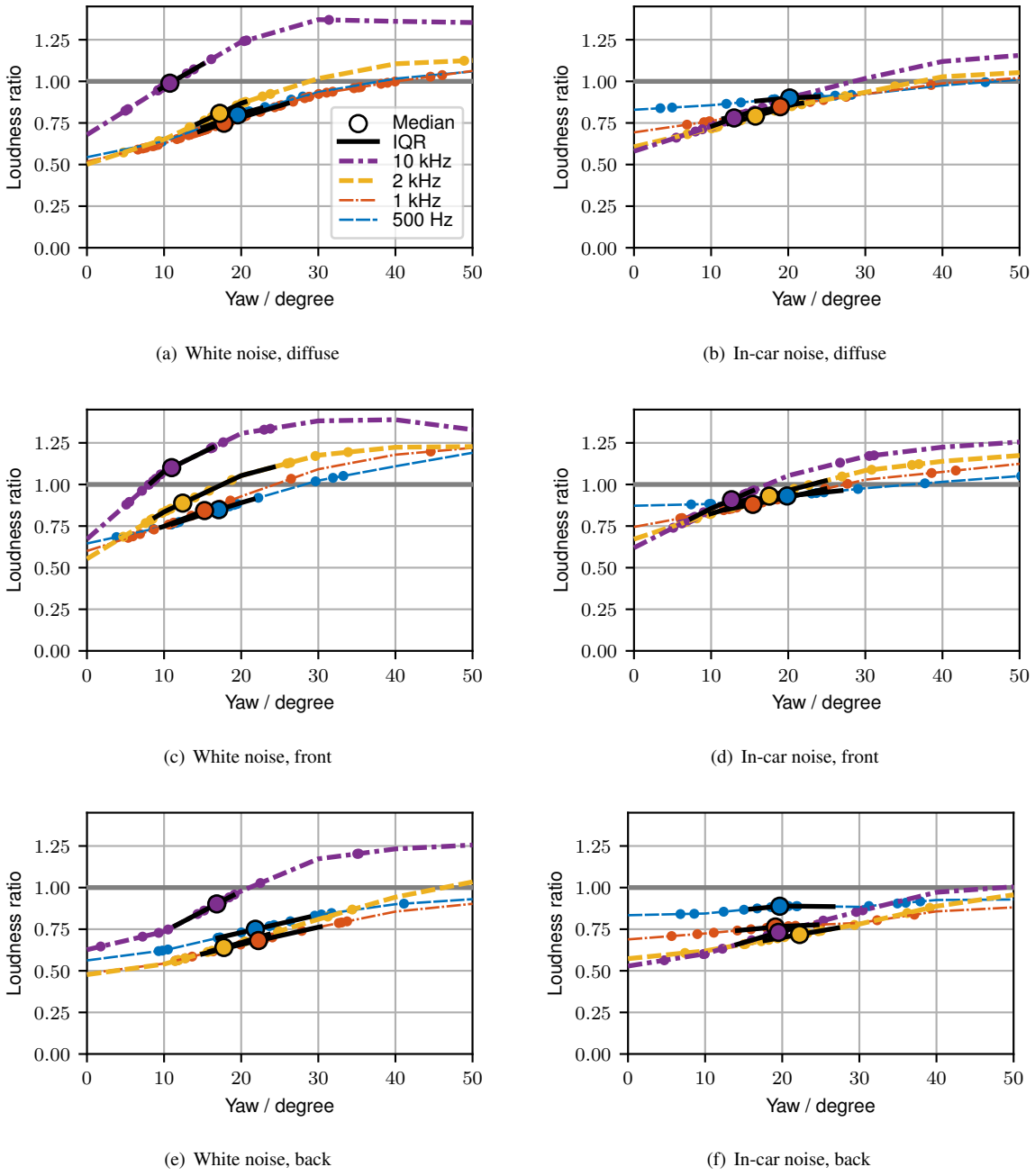

(a) White noise, diffuse

(b) In-car noise, diffuse

(c) White noise, front

(d) In-car noise, front

(e) White noise, back

(f) In-car noise, back

Fig. 10: Relative loudness reduction for different head rotations and cut-off frequencies. Median, range between first and third quartile (IQR), and individual responses are overlaid.

perceived loudness as without ANC. However, the first quartile of responses over all trials with frontal disturbances still lies on average at a ratio of 0.87, comparable to diffuse scenarios.

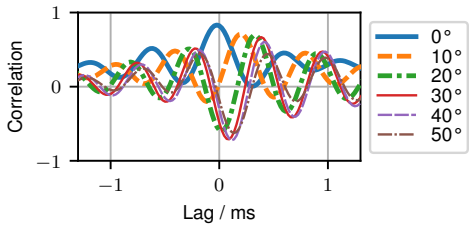

Fig. 11: Interaural cross-correlation function for low-pass filtered dorsal white noise at 2 kHz cut-off frequency with ANC for different head rotations.

Fig. 10 shows that for head rotation similar observations can be made regarding the response behaviour and the noise reduction ratio. The mean of the first quartile is at a slightly lower loudness ratio of 0.77 with a higher standard deviation of 0.1. Results for frontal disturbances (see Fig. 10(c) and 10(d)) are in a similar noise reduction range as the transition trials. The results for diffuse and dorsal disturbances are comparable as well, but tend to have the median response at positions exhibiting more noise reduction than at the corresponding transition trials. It is very likely that a second phenomenon is at play here. Starting at approximately 15 ° head rotation, the ipsilateral secondary speaker can be localised as an independent sound source, potentially confining the perceived extent of the ZoC further. The interaural cross-correlation function [23] (IACF) can act as measure to support this theory. Fig. 11 shows as example the IACF for white, dorsal disturbances with a cut-off frequency at 2 kHz. Even at a small head rotation of 10 °, the IACF begins to collapse. It reaches a plateau with strong negative components near 0 ms lag above 20 ° head rotation, indicating a predominant secondary source at the ipsilateral ear, producing sound with inverted phase compared to the (primary) sound field at the contralateral ear.

6 Conclusion

In the presented study, the perceived spatial extent of local ANC with an active headrest setup is evaluated in a listening experiment. A lateral transition of 2 cm to 4 cm is tolerated by 75 % of the participants. The size of this area decreases with increased controlled bandwidth. Dorsal disturbances typically result in a larger perceived ZoC due to a closer match of phase variation between primary and secondary sources in the tested setup. Results for variable head rotations are in a range of 10 ° to 15 ° for dorsal and diffuse disturbances and 7 ° to 12 ° for frontal disturbances while being relatively independent of controlled bandwidth.

When examining the relative loudness reduction as ratio of the binaural loudness with and without ANC, most answers for dorsal and diffuse scenarios converge at positions with loudness reduction of 20 %. For frontal disturbances and cases with less noise reduction at the reference position, the median response is shifted to positions with less noise reduction. Especially when rotating the head, the distinct perception and localisation of the secondary speaker acts an additional constraint on the size of the ZoC. The connection between the perceived spatial extent of ANC and the loudness reduction can be used in the design process of noise control systems, for example to determine the required accuracy of head-tracking for local noise control.

For this experiment, we considered only a single geometrical setup. To validate the results, future studies may evaluate the extent of the ZoC for different arrangements and with higher spatial resolution. Additionally, numerical simulations of the ANC setup would be of interest to compare the results to the analytical work by Rafaely [9]. However, these simulations would require FEM/BEM approaches towards higher controlled bandwidths [3].

References

[1] Cheer, J., “Active Sound Control in the Automotive Interior,” in A. Fuchs and B. Brandstätter, editors, *Future Interior Concepts*, pp. 53–69, Springer International Publishing, Cham, 2021, ISBN 978-3-030-51044-2, doi:10.1007/978-3-030-51044-2_3.

[2] Olson, H. F. and May, E. G., “Electronic Sound Absorber,” *J. Acoust. Soc. Am.*, 25(6), pp. 1130–1136, 1953, ISSN 0001-4966, doi:10.1121/1.1907249.

[3] Garcia-Bonito, J., Elliott, S. J., and Boucher, C. C., “Generation of Zones of Quiet Using a

Virtual Microphone Arrangement," *J. Acoust. Soc. Am.*, 101(6), pp. 3498–3516, 1997, ISSN 0001-4966, 1520-8524, doi:10.1121/1.418357.

[4] Buck, J. and Sachau, D., "Active Headrests with Selective Delayless Subband Adaptive Filters in an Aircraft Cabin," *Mech. Syst. Signal Process.*, 148, p. 107164, 2021, ISSN 08883270, doi:10.1016/j.ymssp.2020.107164.

[5] Xiao, T., Qiu, X., and Halkon, B., "Ultra-Broadband Local Active Noise Control with Remote Acoustic Sensing," *Sci. Rep.*, 10(1), p. 20784, 2020, ISSN 2045-2322, doi:10.1038/s41598-020-77614-w.

[6] Boucher, C., Elliott, S. J., and Nelson, P. A., "Effect of Errors in the Plant Model on the Performance of Algorithms for Adaptive Feedforward Control," *IEE Proceedings F (Radar and Signal Processing)*, 138(4), p. 313, 1991, ISSN 0956375X, doi:10.1049/ip-f-2.1991.0042.

[7] Elliott, S. J., Joseph, P., Bullmore, A., and Nelson, P. A., "Active Cancellation at a Point in a Pure Tone Diffuse Sound Field," *J. Sound Vib.*, 120(1), pp. 183–189, 1988, ISSN 0022460X, doi:10.1016/0022-460X(88)90343-4.

[8] Elliott, S. J. and Garcia-Bonito, J., "Active Cancellation of Pressure and Pressure Gradient in a Diffuse Sound Field," *J. Sound Vib.*, 186(4), pp. 696–704, 1995, ISSN 0022460X, doi:10.1006/jsvi.1995.0482.

[9] Rafaely, B., "Zones of Quiet in a Broadband Diffuse Sound Field," *J. Acoust. Soc. Am.*, 110(1), pp. 296–302, 2001, ISSN 0001-4966, doi:10.1121/1.1377632.

[10] Jung, W., Elliott, S. J., and Cheer, J., "Combining the Remote Microphone Technique with Head-Tracking for Local Active Sound Control," *J. Acoust. Soc. Am.*, 142(1), pp. 298–307, 2017, ISSN 0001-4966, doi:10.1121/1.4994292.

[11] Holzmüller, F. and Sontacchi, A., "Assessment of the Spatial Extent of Local Active Noise Control - Dataset," 2024, doi:10.5281/zenodo.7756341, "Version 2.0.0".

[12] Elliott, S. J. and Cheer, J., "Modeling Local Active Sound Control with Remote Sensors in Spatially Random Pressure Fields," *J. Acoust. Soc. Am.*, 137(4), pp. 1936–1946, 2015, ISSN 0001-4966, doi:10.1121/1.4916274.

[13] Farina, A., "Simultaneous Measurement of Impulse Response and Distortion with a Swept-Sine Technique," in *AES 108th Convention*, Paris, 2000.

[14] Zhivomirov, H. and Nedelchev, I., "A Method for Signal Stationarity Estimation," *Romanian J. Acoust. Vib.*, 17(2), pp. 149–155, 2020, ISSN 1584-7284.

[15] Gustafsson, F., "Determining the Initial States in Forward-Backward Filtering," *IEEE Trans. Signal Process.*, 44(4), pp. 988–992, 1996, ISSN 1941-0476, doi:10.1109/78.492552.

[16] Riedel, S., Frank, M., and Zotter, F., "The Effect of Temporal and Directional Density on Listener Envelopment," *J. Audio Eng. Soc.*, 71(7/8), pp. 455–467, 2023, ISSN 15494950, doi:10.17743/jaes.2022.0088.

[17] Zotter, F. and Frank, M., "All-Round Ambisonic Panning and Decoding," *J. Audio Eng. Soc.*, 60(10), pp. 807–820, 2012.

[18] Iglesia, D., "The Mobility Is the Message: The Development and Uses of MobMuPlat." in *5th International Pure Data Convention*, New York, 2016.

[19] Tinsley, H. E. and Weiss, D. J., "Interrater Reliability and Agreement of Subjective Judgments." *J. Couns. Psychol.*, 22(4), pp. 358–376, 1975, ISSN 1939-2168, 0022-0167, doi:10.1037/h0076640.

[20] Wilcoxon, F., "Individual Comparisons by Ranking Methods," *Biometrics Bulletin*, 1(6), p. 80, 1945, ISSN 00994987, doi:10.2307/3001968.

[21] Holm, S., "A Simple Sequentially Rejective Multiple Test Procedure," *Scand. J. Stat.*, 6(2), pp. 65–70, 1979, ISSN 0303-6898.

[22] Moore, B. C. J. and Glasberg, B. R., "Modeling Binaural Loudness," *J. Acoust. Soc. Am.*, 121(3), pp. 1604–1612, 2007, ISSN 0001-4966, 1520-8524, doi:10.1121/1.2431331.

[23] ISO/TC 43/SC 2, "ISO 3382-1:2009: Acoustics - Measurement of Room Acoustic Parameters - Part 1: Performance Spaces," 2009.